ACTA ASTRONOMICA
Vol. **54** (2004) pp. 129–152

The Optical Gravitational Lensing Experiment. Small Amplitude Variable Red Giants in the Magellanic Clouds*

by

I. Soszyński[1,2], A. Udalski[1], M. Kubiak[1],
M. Szymański[1], G. Pietrzyński[1,2], K. Żebruń[1],
O. Szewczyk[1] and Ł. Wyrzykowski[1]

[1] Warsaw University Observatory, Al. Ujazdowskie 4, 00-478 Warszawa, Poland
e-mail: (soszynsk,udalski,mk,msz,pietrzyn,zebrun,szewczyk,wyrzykow)@astrouw.edu.pl
[2] Universidad de Concepción, Departamento de Fisica, Casilla 160–C, Concepción, Chile

Received June 12, 2004

ABSTRACT

We present analysis of the large sample of variable red giants from the Large and Small Magellanic Clouds detected during the second phase of the Optical Gravitational Lensing Experiment (OGLE-II) and supplemented with OGLE-III photometry. Comparing pulsation properties of detected objects we find that they constitute two groups with clearly distinct features. In this paper we analyze in detail small amplitude variable red giants (about 15 400 and 3000 objects in the LMC and SMC, respectively). The vast majority of these objects are multi-periodic. At least 30% of them exhibit two modes closely spaced in the power spectrum, what likely indicates non-radial oscillations. About 50% exhibit additional so called Long Secondary Period.

To distinguish between AGB and RGB red giants we compare *PL* diagrams of multi-periodic red giants located above and below the tip of the Red Giant Branch (TRGB). The giants above the TRGB form four parallel ridges in the *PL* diagram. Among much more numerous sample of giants below the TRGB we find objects located on the low luminosity extensions of these ridges, but most of the stars are located on the ridges slightly shifted in $\log P$. We interpret the former as the second ascent AGB red giants and the latter as the first ascent RGB objects. Thus, we empirically show that the pulsating red giants fainter than the TRGB are a mixture of RGB and AGB giants.

Finally, we compare the Petersen diagrams of the LMC, SMC and Galactic bulge variable red giants and find that they are basically identical indicating that the variable red giants in all these different stellar environments share similar pulsation properties.

Key words: *Stars: oscillations – Stars: late-type – Stars: AGB and post-AGB – Magellanic Clouds*

1. Introduction

In recent years a significant progress has been made in studies of pulsations of red giants. The major breakthrough occurred when the large microlensing surveys

*Based on observations obtained with the 1.3 m Warsaw telescope at the Las Campanas Observatory of the Carnegie Institution of Washington.

data of huge samples of these stars spanning several years and all-sky IR surveys photometry became available.

Discovered years ago near-infrared period-luminosity (*PL*) relation for Mira-type stars (*e.g.*, Glass and Lloyd Evans 1981) was extended to semi-regular variables by Wood and Sebo (1996) who showed the second sequence in the $\log P{-}K$ diagram of the long period variables (LPV). Subsequently, Wood *et al.* (1999) analyzing MACHO photometric data of stars in the LMC revolutionized this picture showing five parallel ridges in the *PL* diagram (denoted as A–E). These results were later confirmed by independent studies based on data originated in various projects: EROS+DENIS (Cioni *et al.* 2001), MOA (Noda *et al.* 2002), AGAPEROS+DENIS (Lebzelter, Schultheis and Melchior 2002).

Kiss and Bedding (2003, 2004) used photometric data from the OGLE-II catalog of variable stars (Żebruń *et al.* 2001) supplemented with *K*-band photometry from 2MASS survey to analyze variable red giants in the Magellanic Clouds. They discovered separate *PL* relations of a huge number of variables above and below the tip of the red giant branch (TRGB). They distinguished four ridges in the $\log P{-}K$ plane of the pulsating AGB stars and three sequences of giants fainter than the TRGB. They argued that a substantial fraction of variable giants below the TRGB are in the RGB phase.

Ita *et al.* (2004) presented basically identical, albeit sharper picture of the *K*-band *PL* relation using OGLE-II data and more accurate *K*-band photometry obtained from their SIRIUS IR survey of the Magellanic Clouds. OGLE-II variable red giants were also analyzed by Groenewegen (2004).

Small amplitude variability of red giants has been known for decades. Stebbins and Huffer (1930) surveyed photoelectrically red giants and detected variability of many stars of type M0 and later. They discovered that the cooler the star, the larger the scatter of magnitudes. In recent years this rule was extended to K giants. Edmonds and Gilliland (1996) analyzed HST observations of K giants in the globular cluster 47 Tuc. They found variability with periods of 2–4 days and semi-amplitudes of about 5–15 mmag in K3 and later giants. Other surveys of K giants (Jorissen *et al.* 1997, Henry *et al.* 2000) confirmed that microvariability of these stars is a common feature. Tens of Galactic small amplitude red variable stars were monitored in long term monitoring programs by John Percy (*e.g.*, Percy, Wilson and Henry 2001).

Small amplitude red giants were also detected among huge number of variables in the Galactic bulge. Wray, Eyer and Paczyński (2004) analyzed the periodicity of 200 000 objects from the OGLE-II catalog of variable stars in the Galactic bulge (Woźniak *et al.* 2002). They selected 18,000 stars (calling them OGLE Small Amplitude Red Giants – OSARGs) with periods $10 < P < 100$ days and *I*-band amplitudes in the range $0.005 < A < 0.13$ mag. The variables clearly followed two distinct period–amplitude relations.

The nature of small amplitude pulsations of red giants is still not clear. Two mechanisms are proposed: self excitations of unstable modes (so called Mira-like pulsations) and convection induced excitation of linearly stable modes (solar-like oscillations). Both possibilities were discussed by Dziembowski *et al.* (2001) and Christensen-Dalsgaard *et al.* (2001).

One of the by-products of the OGLE survey is a huge number of variable stars found in the Magellanic Clouds. The main purpose of this paper is to provide possibly most precise characteristics of poorly known type of pulsating stars – OGLE Small Amplitude Red Giants in the Large and Small Magellanic Clouds.

2. Observations and Data Reductions

All observations presented in this paper were carried out during the second and the third phases of the OGLE experiment with the 1.3-m Warsaw telescope at Las Campanas Observatory, Chile. The observatory is operated by the Carnegie Institution of Washington. The OGLE-II project started in January 1997. The telescope was equipped with the "first generation" camera with a SITe 2048×2048 CCD detector working in drift-scan mode. The pixel size was 24 μm giving the 0.417 arcsec/pixel scale. Observations were performed in the "slow" reading mode of the CCD detector with the gain 3.8 e^-/ADU and readout noise of about 5.4 e^-. For details of the instrumentation setup of OGLE-II, we refer the reader to Udalski, Kubiak and Szymański (1997). The OGLE-II fields cover 4.5 square degrees in the central parts of the LMC and 2.4 square degrees in the SMC.

Second phase of the OGLE project was completed in November 2000 and in June 2001 the third stage of the experiment began. The Warsaw telescope was equipped with a "second generation" CCD mosaic camera consisting of eight SITe ST-002a CCD detectors with 2048×4096 pixels of 15 μm size (Udalski 2003a). This corresponds to 0.26 arcsec/pixel scale and the field of view of the whole mosaic $35' \times 35'$. The last observations presented in this paper were collected in November 2003, so the analyzed data span 8 years.

Photometry was obtained with *I* and *V* filters, closely resembling the standard system. For the period analysis *I*-band observations were used, in which the majority of frames were taken. The OGLE-II photometry was obtained using the Difference Image Analysis (DIA) method – image subtraction algorithm developed by Alard and Lupton (1998) and Alard (2000), and implemented by Woźniak (2000). Contrary to the general catalog of variable stars in the Magellanic Clouds (Żebruń *et al.* 2001), the DIA photometry was reprocessed for all stars found in the reference images of the fields. In this way more complete sample, in particular of very small amplitude variable red giants, could be detected among monitored stars. The OGLE-III photometry comes from the standard OGLE-III photometry pipeline (Udalski 2003a) and is also based on DIA.

We tied photometry obtained during the second and third phases of the OGLE survey by shifting the OGLE-III magnitudes to well calibrated OGLE-II photometry. For each object we determined the median difference between OGLE-III and OGLE-II luminosities of at least several dozen constant stars in the closest neighborhood. This value was then used as the correction of the OGLE-III magnitudes. Combined OGLE-II and OGLE-III datasets with its much longer time span made it possible to derive much more complete and accurate periodicities by filtering out spurious, non-coherent and unstable frequencies possible in the OGLE-II dataset alone.

Altogether, we collected from about 400 to 800 observations in *I* filter (depending on the field) and about 30–70 measurements in the *V*-band. In the OGLE-II phase the effective exposure time lasted 125 and 174 seconds for the *I* and *V*-band, respectively. OGLE-III exposure time of observations in *I*-band was increased to 180 seconds. The median seeing of our dataset was about $1\overset{\prime\prime}{.}3$.

In the majority of other analysis of red giant pulsations near infrared photometric bands were used, especially *K*-band magnitudes. Stars in the latest phases of evolution are characterized by the high mass-loss, and they are often obscured by significant amount of dust. Therefore, infrared bands minimize the scatter of the *PL* sequences caused by interstellar extinction. On the other hand infrared magnitudes usually come from single epoch measurements what increases the scatter.

We used in our analysis reddening free Wesenheit index, W_I, defined as:

$$W_I = I - 1.55(V - I)$$

where *I* and *V* are intensity mean magnitudes and 1.55 is the mean ratio of total-to-selective absorption $(A_I/E(V-I))$. It is worth noticing that the *PL* diagrams which use W_I index present sequences fairly narrow, similar or even better defined than in the $\log P$–K diagrams.

3. Selection of OSARGs

We searched for variable red giants among *I*-band light curves of all stars brighter than 17 mag and 17.5 mag in the LMC and SMC, respectively. Usually, a search for variable stars is preceded by a preliminary selection based, for instance, on scatter of observations. However, we performed the period analysis of each star, because substantial number of small amplitude variable red giants could have been rejected during the preselection process.

At the first stage of the search we performed a low-resolution period analysis of about 260 000 and 120 000 objects in the LMC and SMC, respectively. We used program FNPEAKS (Kołaczkowski 2003, private communication) which implements the algorithm of Discrete Fourier Transform.

After selection of the highest peak in the power spectrum corresponding to the primary dominant period we examined periodograms with higher resolution and determined more accurate primary periods. Then, the light curve of analyzed object was folded with derived period, approximated by third order Fourier series and fitted functions were subtracted from the observational data. The residuals were again searched for other periodic signal by repeating the procedure. Only periods with the signal-to-noise parameter larger than 3.6 were considered as real. Up to five dominant periods per object were kept. Finally, all objects with no *V*-band measurements and stars with colors $V-I<1.0$ (*e.g.*, Cepheids, main sequence stars) were rejected.

The input list of stars consisted of both, variable and non-variable, objects. Separation of red giants with the smallest amplitudes from non-variable stars turned out to be quite difficult. In some cases neither the scatter of the measurements, nor signal-to-noise parameter produced by the period searching program, nor even visual inspection of the light curves, allowed to distinguish between variables and non-variables. Therefore, for each object we performed a second periodicity search using another program, PREDATOR, (Mizerski 2004, private communication) based on another method of the frequency analysis (Lomb-Scargle algorithm). For further studies we limited our sample to stars which the dominant period derived during the first search was found between 25 highest peaks of the periodogram obtained in the second stage. This method allowed us to reject the vast majority of non-variable objects.

The vast majority of the selected small amplitude variables are multi-periodic. Certainly, a small part of periods derived in stars from our sample might be spurious. This is inevitable when analyzing light curves of variables with so small amplitudes. However, the visual inspection of light curves indicates, that the vast majority of variables have dominant periods well determined, what combined with large number of objects in the final sample enabled us to study statistical features of variable red giants.

In the upper panels in Fig. 1 we show the *PL* relation, $\log P - W_I$, for our sample of variable red giants in the LMC. Only primary periods with signal-to-noise parameter larger than 6 are presented: altogether 16 000 stars. *PL* diagram showing several clear well separated sequences of pulsating red giants is basically identical with infrared diagram for the *K*-band (Ita *et al.* 2004). We labeled the ridges A–D following notation of Wood *et al.* (1999), adding label C$''$ for a clear sequence between C and D, weakly seen in the *K*-band (Ita *et al.* 2004). The sequence denoted as C$'$ by Ita *et al.* (2004) is practically merged with the ridge B in Fig. 1.

Lower panels in Fig. 1 show the *PL* relations constructed using the second and third dominant periods of stars highlighted in magenta in the upper panels, that is the sequence A (3800 objects) in the left diagram, and sequence C (1400 objects) in the right diagram. As can be noticed, both groups of red giants form completely different patterns in the secondary period–W_I plane. Stars with the primary periods in the sequence A reveal four narrow *PL* ridges corresponding to the sequences A and B, and additional wider sequence corresponding to the sequence D. Sequences C and C$''$ are not present at all in the bottom-left plot in Fig. 1.

On the other hand, stars with the primary periods located in the sequence C

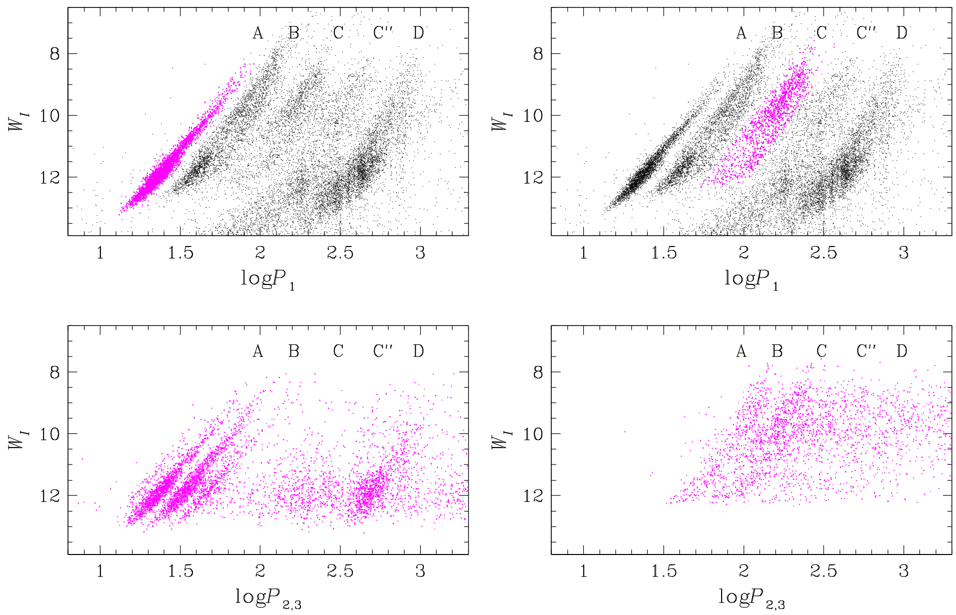

Fig. 1. Period–W_I diagrams for variable red giants in the LMC. The upper diagrams are constructed using primary periods with $S/N>6$. The lower diagrams show the second and third dominant periods–W_I relation for giants from the ridge A (*left panel*) and C (*right panel*).

also form clear ridges in the bottom-right panel of Fig. 1. They correspond to the sequences B, C and less clearly C$''$. The ridge D is practically not seen in this panel. It is also evident that none of the secondary periods of this group correspond to the sequence A.

This striking difference between variable giants belonging to ridges A and C suggests that both groups represent different types of pulsating stars. The first group is referred in this paper as OSARG. The second group of long period variables (LPV), consisting of semi-regular variables (SRV) and Mira type variables, will be analyzed in a forthcoming paper. It is worth noticing here that in both groups of stars many secondary periodicities are very close to the primary ones (*i.e.*, stars with primary periods in the ridge A or C have other dominant periods in the ridge A or C, respectively, as well) suggesting non-radial pulsations of these objects (see Section 4 and 5).

Sequence B (2500 objects) in the upper panels of Fig. 1 must contain both types of pulsating giants: OSARG and SRV/Mira stars because this ridge is populated in both bottom panels of Fig. 1. To separate these groups we used the second and next (if present) dominant periods. If one of these periods fell into the sequence A, we classified such an object as OSARG. Otherwise, the star was added to the list of SRV/Mira objects.

Left panels in Fig. 2 show properties of OSARGs with the primary periods in the ridge B. Right panels present the same diagrams for SRV/Mira variables. In the

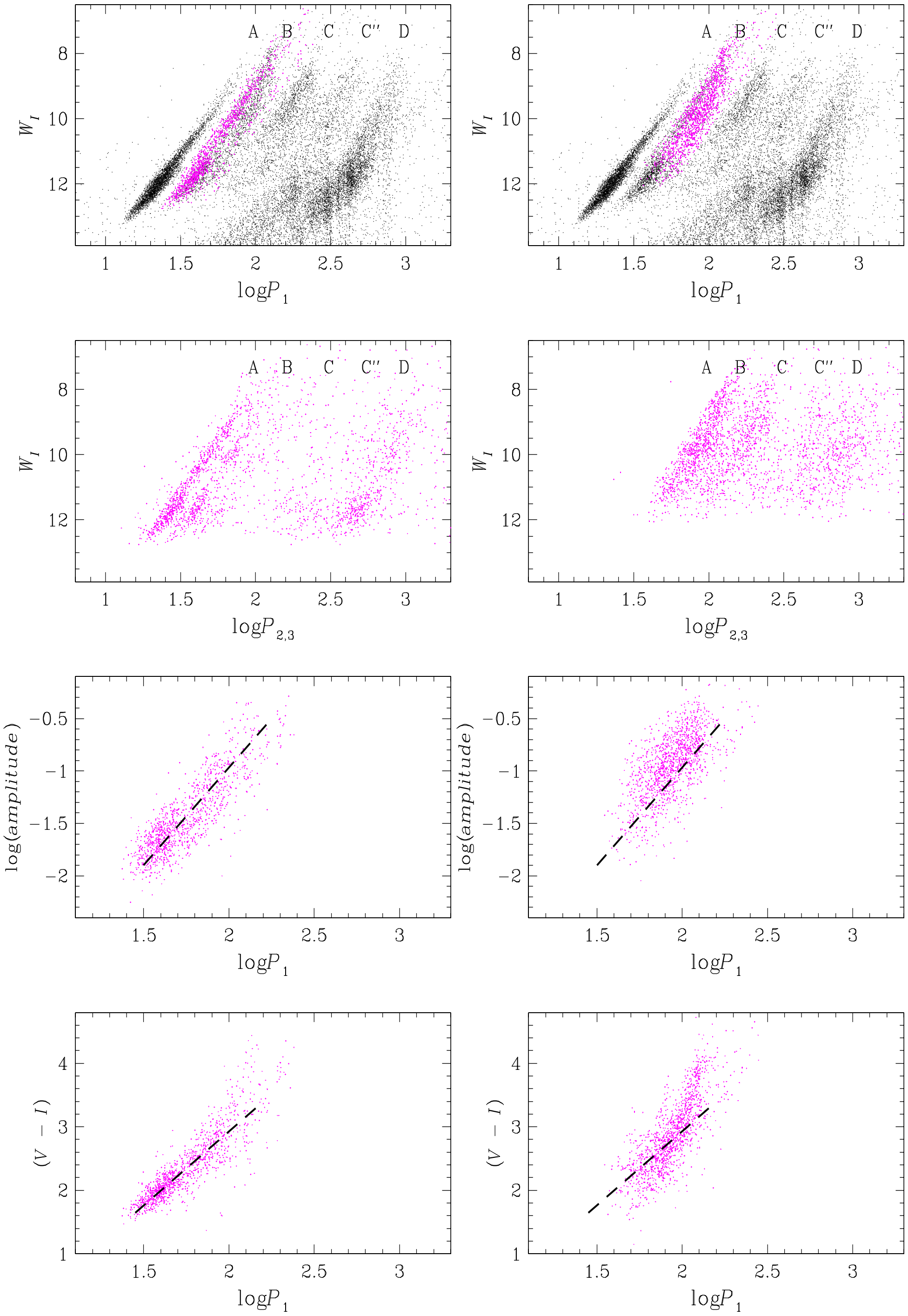

Fig. 2. The top panels present the primary period–W_I relation for variable red giants in the LMC (Fig. 1). The next rows show as follows: secondary periods–W_I relation, period–amplitude (I-band) relation and period–color $(V-I)$ relation for stars highlighted in magenta in the top panels. Least square fits for period–amplitude and period–color relation of stars in the left column are repeated for comparison in appropriate panels of the right column.

top row *PL* relations of the primary dominant periods are repeated with OSARGs (left) or SRV/Mira stars (right) highlighted in magenta.

In the next row of Fig. 2 *PL* diagrams for other dominant periods are presented. It is clearly seen that the secondary periods of SRV/Mira objects populate mostly sequences B (its part denoted as C$'$ by Ita *et al.* 2004) and C similar to objects with the primary periods in the ridge C (right panels in Fig. 1). On the other hand the secondary periods of stars from the ridge B classified as OSARGs closely follow the pattern of stars with primary periods in the sequence A (left panels in Fig. 1). Thus, we indeed see that the ridge B for primary periods is a mixture of OSARG and SRV/Mira variables – stars with different pulsational properties. Our criterion of classification seems to properly separate stars belonging to both groups.

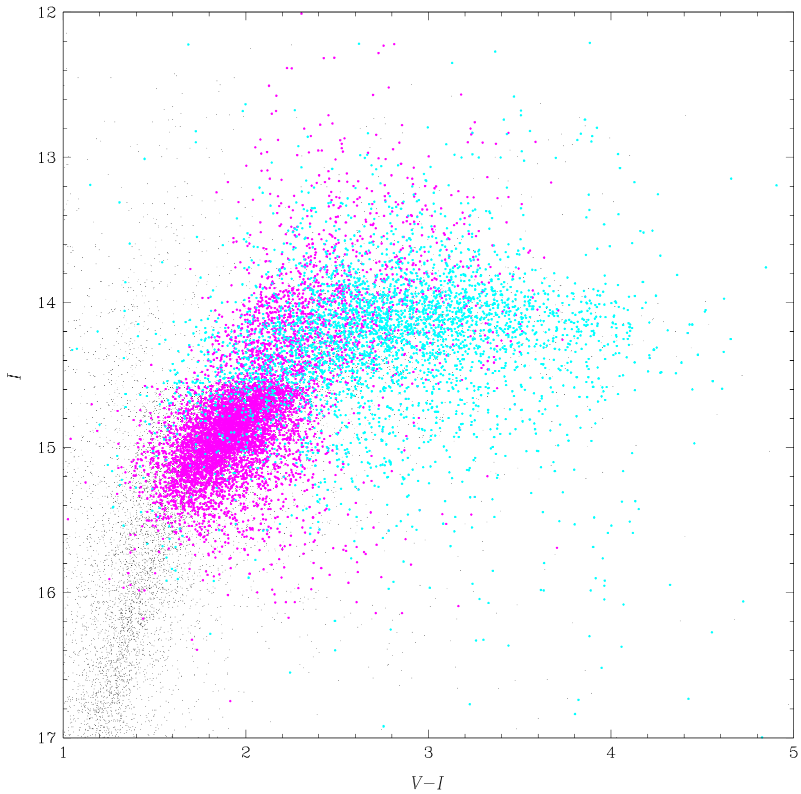

Fig. 3. Color-magnitude diagram of the LMC red giants. Objects classified as OSARGs are plotted in magenta and SRV/Mira stars in cyan.

The period–amplitude and period–color diagrams for stars with primary period in the ridge B, presented in the consecutive rows in Fig. 2, reveal that though the ranges of the amplitudes and colors of both groups of variables overlap, they follow distinct $\log P$–A and $\log P$–$(V-I)$ relations. The SRV/Mira objects typically have larger amplitudes and span wider range of colors. All these features also suggest that OSARG and SRV/Mira variables are different types of pulsating stars.

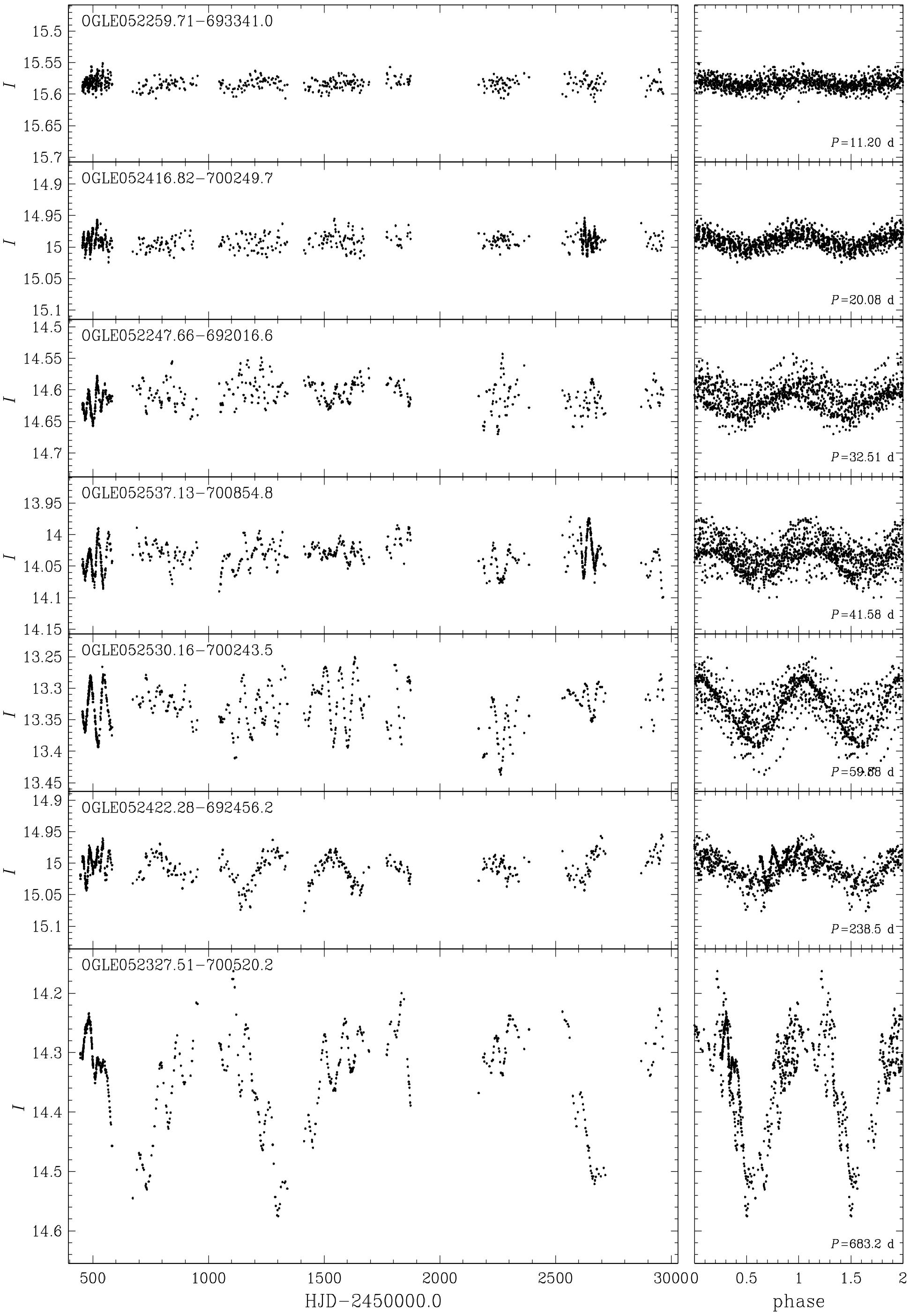

Fig. 4. Examples of the light curves of the OSARG objects in the LMC. In the first three upper rows light curves of OSARGs fainter than the TRGB are presented. In the next two rows examples of OSARGs above the TRGB are shown. Bottom two rows present variables with distinct long secondary periods.

Similar test performed on variable red giants that have the primary periods in the ridge D in Fig. 1 indicates that this group is also a mixture of OSARG and SRV/Mira stars, *i.e.*, the former have dominant periodicities in the ridge A while the latter do not.

Fig. 3 presents the color–magnitude diagram of the LMC stars. Only the upper part of the red giant branch is shown. Objects classified as OSARG and SRV/Mira are plotted in magenta and cyan, respectively.

Fig. 4 shows eight typical light curves of OSARGs in the LMC. The original data (left panel) and folded light curves (right panel) are arranged according to periods. To compare amplitudes of variability all diagrams have the same magnitude scale. Three upper light curves present typical OSARGs below the TRGB, next two rows show giants brighter than the TRGB, two lowest light curves are examples of stars with long secondary periods (see below).

4. OSARGs above the TRGB

Kiss and Bedding (2003) found a clear drop of stellar density of variable red giants above the TRGB. They also noticed that *PL* relations of giants brighter and fainter than the TRGB are shifted by about $\Delta \log P \approx 0.05$. Therefore, we separated our sample of OSARGs into two groups, namely the stars above and below the TRGB and analyzed them separately. Detailed studies of the multi-periodic stars revealed significant differences between both groups. Hereafter we refer OSARGs brighter than the TRGB as type "a" (for "above TRGB") with the sequence number (*e.g.*, a_1 means the sequence with the longest periods). Objects fainter than the TRGB will be described by letter "b" (for "below TRGB") with the appropriate sequence number.

We used *I*-band magnitudes of the TRGB determined by Udalski (2000): $I_{\rm TRGB} = 14.56$ mag in the LMC, and $I_{\rm TRGB} = 14.95$ mag in the SMC to separate the stars. Fig. 5 shows the $\log P{-}W_I$ *PL* relation of the OSARGs above the TRGB in the LMC and SMC (about 2000 and 400 objects, respectively). For each star up to four points representing the primary and next three dominant periods are marked. Four distinct sequences, labeled $a_1 - a_4$, are clearly visible in the *PL* relations of both galaxies.

Sequence a_3 corresponds to the ridge A of Wood *et al.* (1999) while sequences a_2 and a_1 were merged in their ridge B (Fig. 1). Poorly populated ridge a_4 has not been noticed in earlier analyses. Sequence a_3 is the most numerous in the LMC and SMC. Primary periods of almost half of the OSARGs of type "a" populate sequence a_3 but for further 40% of stars one of the next dominant periods also corresponds to this sequence. About 20% of primary periods of OSARGs fall into the sequence a_2, and only a few percents of the variables have the primary periods in the sequences a_1 and a_4. The remaining OSARGs above the TRGB exhibit the dominant periodicity in the sequence of long secondary periods (LSP).

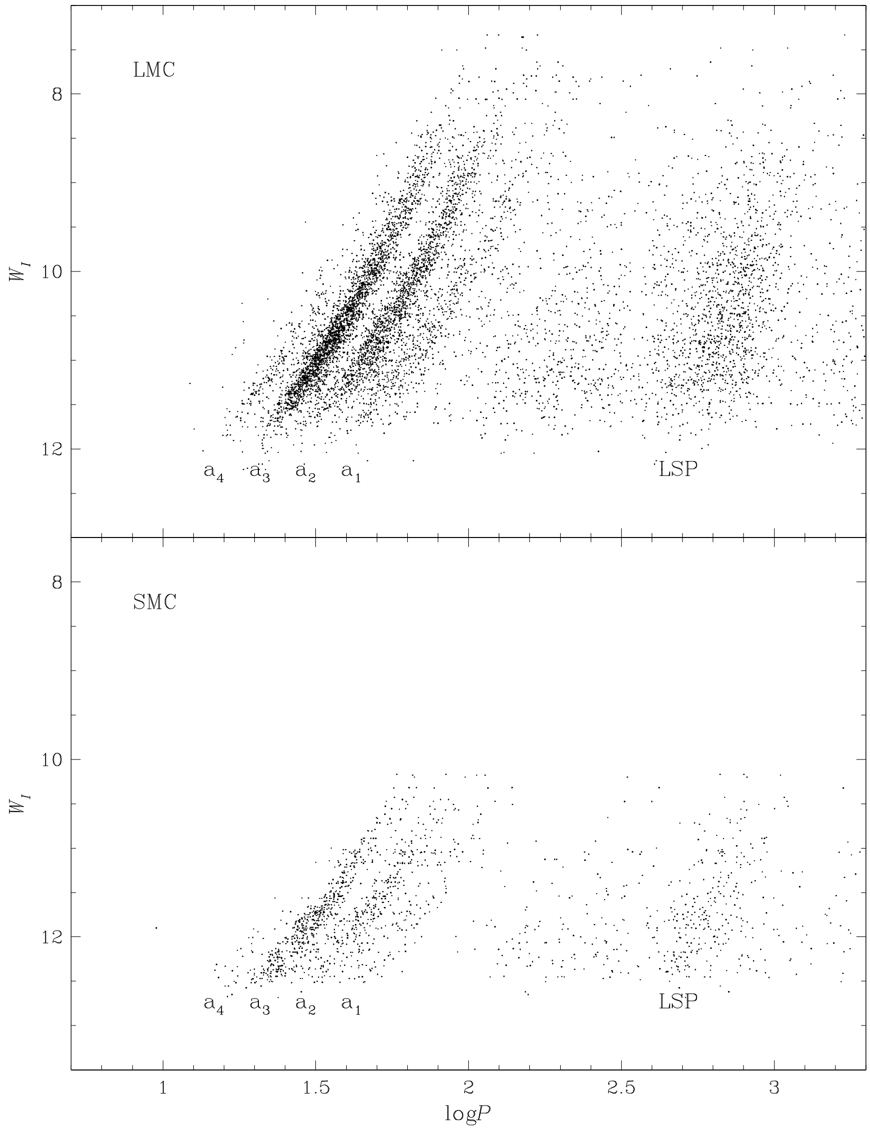

Fig. 5. Period-W_I diagrams for OSARG stars brighter than the TRGB in the LMC (upper panel) and SMC (lower panel). Up to four dominant periods for each star are plotted.

Fig. 5 indicates that the *PL* relations for W_I index of OSARGs brighter than the TRGB are not linear. The slope becomes steeper for brighter W_I indices. It is worth noticing that the slope of the *PL* relations is different in the LMC and SMC, namely it is steeper in the LMC than in the SMC.

Fig. 6 presents the Petersen diagram of OSARG stars from the LMC located above the TRGB, that is a diagram where the period ratio of two periods in a multi-period object is plotted against logarithm of the longer period. Period ratios of all combinations of up to four dominant periods in each object were plotted in the top panel of Fig. 6.

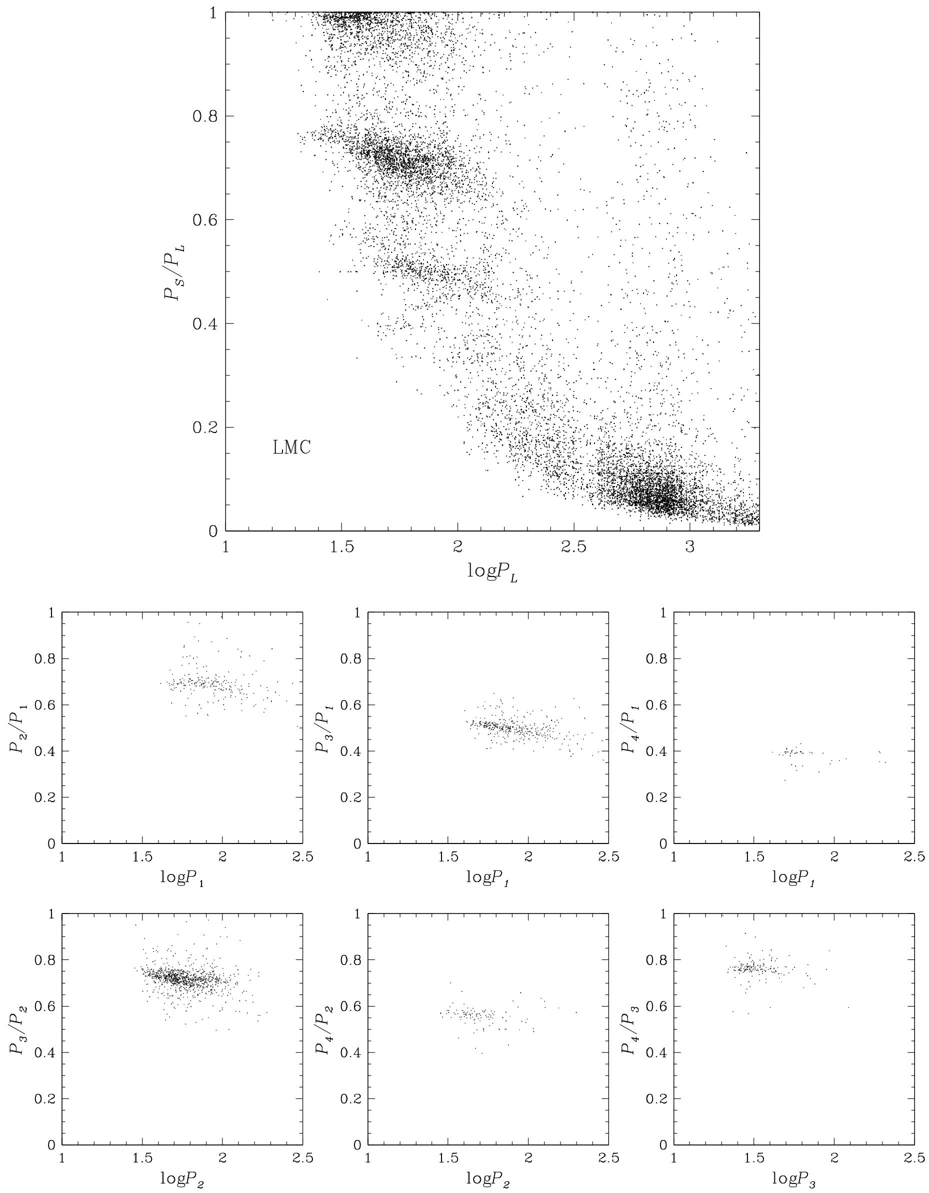

Fig. 6. Petersen diagram for OSARG stars brighter than the TRGB in the LMC. The large panel present ratios of the four dominant periods of all these stars. The small diagrams present objects pulsating with periods located in the four sequences in the *PL* diagram (Fig. 5).

Six smaller panels present the Petersen diagrams for objects that possess periods in the four sequences, $a_1 - a_4$, in the *PL* diagram. For example, in the left-top panel the ratios of the periods for objects that pulsate simultaneously with periodicities falling into sequence a_1 and a_2 are presented. All combinations of sequences are shown. One can easily find a characteristic period ratio of the sequences and its dependence on period.

It can be noted from Fig. 6 that the considerable fraction of the points in the Petersen diagram is located in the region of period ratios larger than 0.97. Such very closely spaced frequencies were also detected in other types of pulsating stars, *e.g.*, RR Lyr variables (Olech *et al.* 1999) or Cepheids (Moskalik, Kołaczkowski and Mizerski 2003), and were interpreted as an indication of non-radial oscillations. By analogy we suppose that these objects also pulsate non-radially.

The phenomenon of close periodicities is very common in OSARGs. For about 35% of OSARGs in the LMC and 30% in the SMC we found two (or more) close frequencies between five highest peaks in the periodograms. More detailed analysis of the periodograms would probably significantly increase the number of stars oscillating in non-radial modes.

In about 55% of OSARGs long secondary periods (LSP, Houck 1963), *i.e.*, periods typically 5–15 times longer than primary periods, were detected. A clump of points representing these periodicities is clearly visible in the lower-right part of the Petersen diagram. For about half of the stars exhibiting LSP, amplitudes of the long period variability are larger than amplitudes of typical OSARG's pulsation modes – see an example in the bottom panel of Fig. 4. However, the behavior of other periodicities in these stars, like their period ratios, is similar to other OSARGs. Therefore we believe that these objects constitute a common group with typical OSARG stars.

It is worth noticing that LSPs fall into distinct *PL* sequence in Fig. 5, roughly consistent with the sequence D of Wood *et al.* (1999). The origin of the LSP phenomenon is still unknown. Possible explanations include "strange" modes of pulsation, rotation of spotted star, episodic dust ejections, or eclipses of giant by a cloud of dust and gas surrounding the orbiting companion. More details concerning LSP objects are presented by Wood, Olivier and Kawaler (2004).

Finally, the Petersen diagrams made it possible to measure the typical ratio of periods corresponding to different sequences, $a_1 - a_4$, in the *PL* diagram. We obtained the following average values:

$$\begin{aligned}
&P_2/P_1 \approx 0.69 \\
&P_3/P_1 \approx 0.50 \qquad (P_3/P_1 = -0.13 \cdot \log P_1 + 0.74) \\
&P_4/P_2 \approx 0.39 \\
&P_3/P_2 \approx 0.73 \qquad (P_3/P_2 = -0.13 \cdot \log P_2 + 0.96) \\
&P_4/P_2 \approx 0.56 \\
&P_4/P_3 \approx 0.76
\end{aligned}$$

One can notice that in some cases the period ratio depends on the period. Typically, the longer period, the smaller period ratio. In the case of P_3/P_1 and P_3/P_2 we provide above linear approximations of these relations.

5. OSARGs below the TRGB

The nature of pulsating giants below the TRGB is still not clear. Alves *et al.* (1998) and Wood (2000) argued that all these stars are thermally pulsing AGB stars, while Ita *et al.* (2002) suggested that substantial fraction of these objects are the first ascent RGB stars. Kiss and Bedding (2003) provided additional arguments supporting this hypothesis. They noted that the *PL* relations of variables above and below the TRGB show a relative shift of about $\Delta\log P \approx 0.05$, what is consistent with the evolutionary temperature difference between AGB and RGB stars with luminosities around the TRGB.

Our analysis of multi-periodic variable red giants provides evidences supporting the hypothesis that below the TRGB both: AGB and RGB pulsating stars are observed. Moreover, we attempted to identify samples of first- and second-ascent red giants fainter than the TRGB.

OSARGs below the TRGB are much more numerous than variables above the TRGB. Our sample consists of about 13 400 stars fainter than the TRGB in the LMC and 2600 such objects in the SMC. Fig. 7 presents the $\log P$–W_I diagram, for this group of stars from the LMC and SMC. Similarly to OSARGs brighter than the TRGB four clear *PL* ridges labeled from b_1 to b_4, can be distinguished as well as the sequence of LSPs. The sequences denoted as R_1, R_2 and R_3 by Kiss and Bedding (2003) below the TRGB correspond to the sequences b_1, b_2 and b_3, respectively, while the sequences A^- and B^- of Ita *et al.* (2004) correspond to the sequences b_3 and b_2, respectively.

The $\log P$–W_I relations of OSARGs below the TRGB (Fig. 7) are approximately linear and parallel. The slope of the relation in the SMC is significantly smaller than in the LMC. Using the least square method we fitted the slopes of -5.21 ± 0.05 and -4.15 ± 0.05 for OSARGs of type "b" in the LMC and SMC, respectively. In Table 1 the corresponding zero points of the relation for the sequences $b_1 - b_4$ in the $\log P$–W_I plane are listed for the LMC and SMC. For comparison, the zero points of OSARGs brighter than the TRGB fitted with the same slopes for objects with $W_I > 10$ and $W_I > 11$ for the LMC and SMC, respectively, are also listed (for brighter stars the slopes become steeper).

In further analysis of properties of OSARGs we limited ourselves to the LMC red giants only, as this sample is the most numerous and the data are most accurate. Fig. 8 presents the $\log P$–W_I diagram for all OSARG objects from Figs. 5 and 7 plotted together. The stars brighter than the TRGB are marked with cyan dots. It is clear from Fig. 8 that the ridges of these stars, $a_1 - a_3$, are shifted in $\log P$ relative to the corresponding ridges of stars fainter than the TRGB: $b_1 - b_3$, as noted by Kiss and Bedding (2003).

The location of the sequence indexed by 4, that went unnoticed in Kiss and Bedding (2003) and Ita *et al.* (2004), indicates, however, that the ridge of stars fainter than the TRGB, b_4, is a straight extension of the sequence a_4 of OSARGs brighter than the TRGB, *i.e.*, AGB stars. Fig. 9 shows the distribution of $\log P$ after

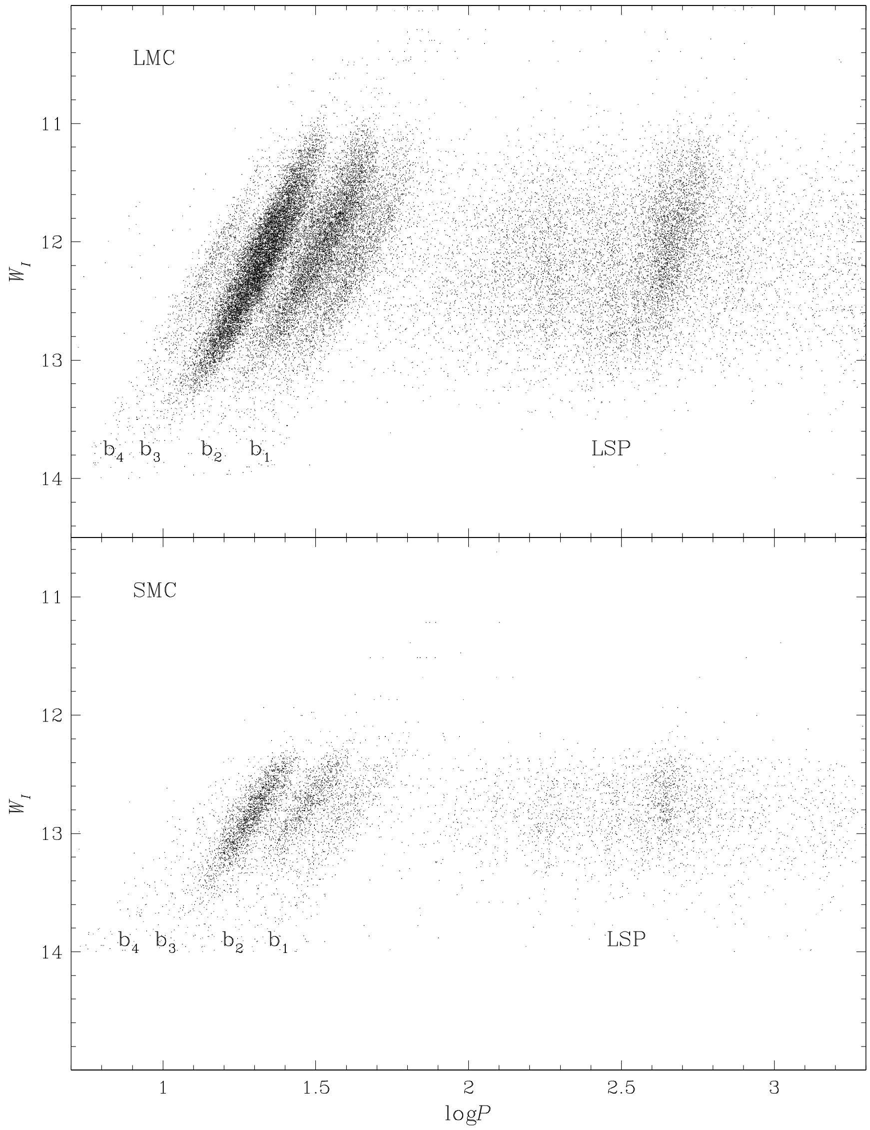

Fig. 7. Period–W_I diagrams for OSARG stars fainter than the TRGB in the LMC (upper panel) and SMC (lower panel). Up to four dominant periods for each star are plotted.

subtraction of the average linear fit for the sequence a_1 (plotted with the broken line in Fig. 8) for the red giants brighter (panel A) and fainter (panel B) than the TRGB. Shifts and coincidence of ridges indexed by 1–3 and 4, respectively, are again clearly seen. Therefore we suspect that the stars fainter than the TRGB with one of the dominant periods in the sequence b_4 constitute the same type stars as those in sequence a_4, *i.e.*, the second ascent AGB red giants.

To verify our hypothesis we closer examined the group of OSARGs fainter than the TRGB with one of the periods located in the sequence b_4. The four dominant

Table 1

Zero points of the $\log P - W_I$ relations

Red Giants brighter than the TRGB				
Sequence	a_1	a_2	a_3	a_4
LMC	20.37	19.59	18.86	18.21
SMC	19.26	18.59	18.01	17.48
Red Giants fainter than the TRGB				
Sequence	b_1	b_2	b_3	b_4
LMC	20.65	19.91	19.07	–
SMC	19.52	18.88	18.22	–

periods of these objects are marked by magenta dots in the *PL* diagram (Fig. 8). The distribution of $\log P$ is also presented in panel C of Fig. 9.

It can be immediately noticed from Figs. 8 and 9 that the dominant periods of red giants from the sequence b_4 form clear three additional ridges in the *PL* diagram corresponding to those indexed by 1–3. What more important these additional ridges are clearly shifted in $\log P$ compared to the ridges of the remaining OSARGs fainter than the TRGB (black dots in Fig. 8). On the other hand they coincide perfectly with the ridges $a_1 - a_3$ of giants brighter than the TRGB, *i.e.*, AGB stars and are the extensions of the AGB stars ridges toward fainter objects. Therefore we believe that the stars possessing the periods in the sequence b_4 are indeed the pulsating red giants on the second ascent.

Fig. 10 shows the Petersen diagram for our group of pulsating AGB giants fainter than the TRGB. The similarities with the diagram of AGB stars brighter than the TRGB presented in Fig. 6 are striking. The period ratio sequences presented in the small panels of Fig. 6 are long-period continuations of the sequences of AGB red giants fainter than the TRGB presented in Fig. 10.

The black dots in Fig. 8 mark the red giants fainter than the TRGB with the dominant periods populating sequences $b_1 - b_3$. We suppose that the vast majority of these stars are the first ascent red giants, *i.e.*, RGB giants (hereafter RGB sample). However, this sample can still be contaminated to some extent by AGB stars. Although we already extracted a group of AGB stars, based on the presence of b_4 sequence periodicity, it cannot be excluded that a number of AGB stars that do not excite this mode of pulsation is still hidden among objects marked by black dots. Unfortunately, the natural width of the *PL* sequences, accuracy of observations and relatively similar distances in $\log P$ between sequences indexed by 1–3 of the AGB and RGB stars make separation of additional AGB stars impossible.

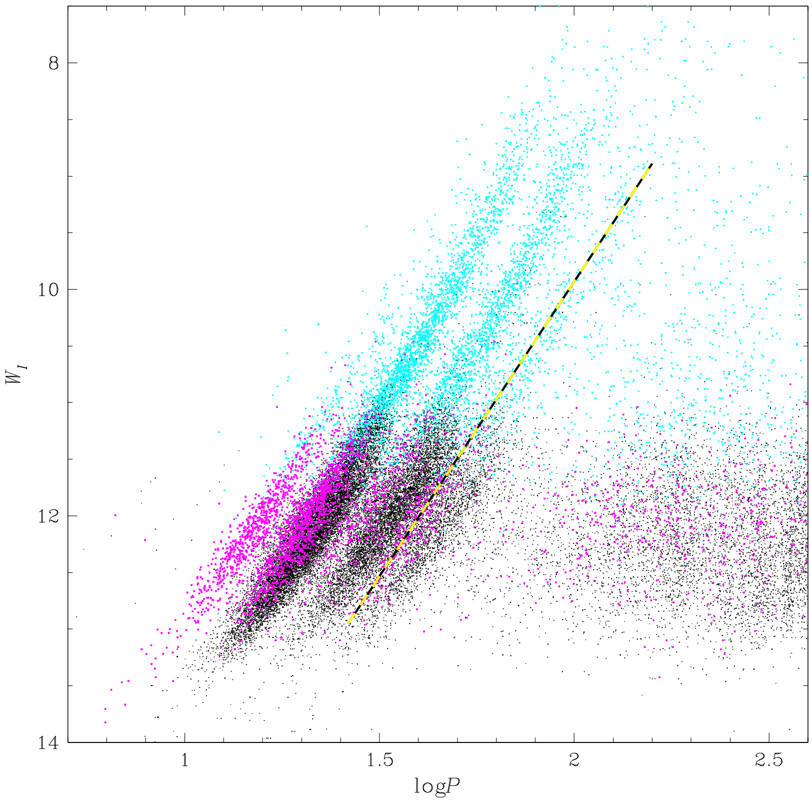

Fig. 8. Period–W_I diagram for all OSARG stars in the LMC. Cyan dots mark OSARGs brighter than the TRGB (AGB stars), black dots OSARGs fainter than the TRGB (RGB sample). Magenta points show the objects with one of the dominant periods belonging to the shortest period sequence b_4, *i.e.*, AGB stars fainter than the TRGB. Broken line is the linear fit to the sequence a_1.

On the other hand the contamination of the RGB sample by hidden AGB stars cannot be large. Panel D of Fig. 9 shows the distribution of $\log P$ of the RGB sample. The expected maxima of the distribution of $\log P$ of AGB stars (marked by vertical lines) are considerably shifted and fall between the maxima of the RGB sample. If the number of AGB stars in the RGB sample were considerable then the minima would be filled and much less pronounced than seen in panel D of Fig. 9. Therefore, we conclude that our RGB sample indeed constitutes in the statistical sense the RGB giants group.

Fig. 11 presents the Petersen diagram of the RGB sample. Similarly to stars located above the TRGB, non-radial pulsations (period ratio close to 1.0) and LSPs (period ratio smaller than 0.2) can be distinguished in Fig. 11 in addition to the clear sequences corresponding to the period ratio of all combinations of periods of sequences $b_1 - b_3$. *PL* relation of the LSP is a continuation of the LSP sequence of stars located above the TRGB (*cf.* Figs. 5 and 7), and overlaps with the sequence D of Wood *et al.* (1999). Both period ratios – close to 1.0 and LSP – are also present in the Petersen diagram of the AGB stars fainter than the TRGB (Fig. 10).

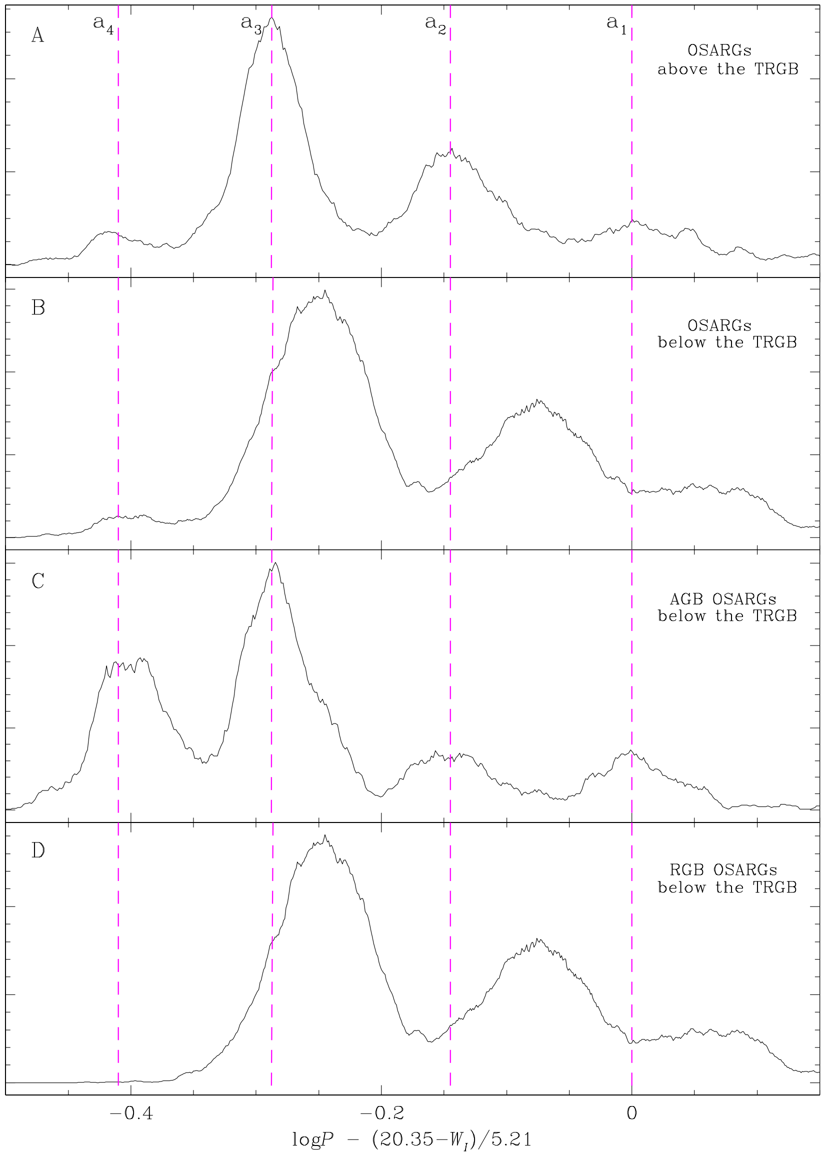

Fig. 9. Distribution of $\log P$ after subtraction of the a_1 sequence fit. *Panel A*: OSARG stars brighter than the TRGB; *panel B*: All OSARG stars fainter than the TRGB; *panel C*: AGB sample of OSARG stars fainter than the TRGB; *panel D*: RGB sample of stars fainter than the TRGB. Vertical dashed lines mark position of sequences $a_1 - a_4$.

A new feature clearly seen in the Petersen diagram in Fig. 11 are the sequences corresponding to the period ratios of about 0.9 and 0.95. These ratios are only observed among objects possessing pulsations in the sequence b_3. The periodicities responsible for these two features form additional sequences in the *PL* diagram merged with the ridge of b_3 in Figs. 7 and 8 and, thus, additionally widening it compared to other ridges.

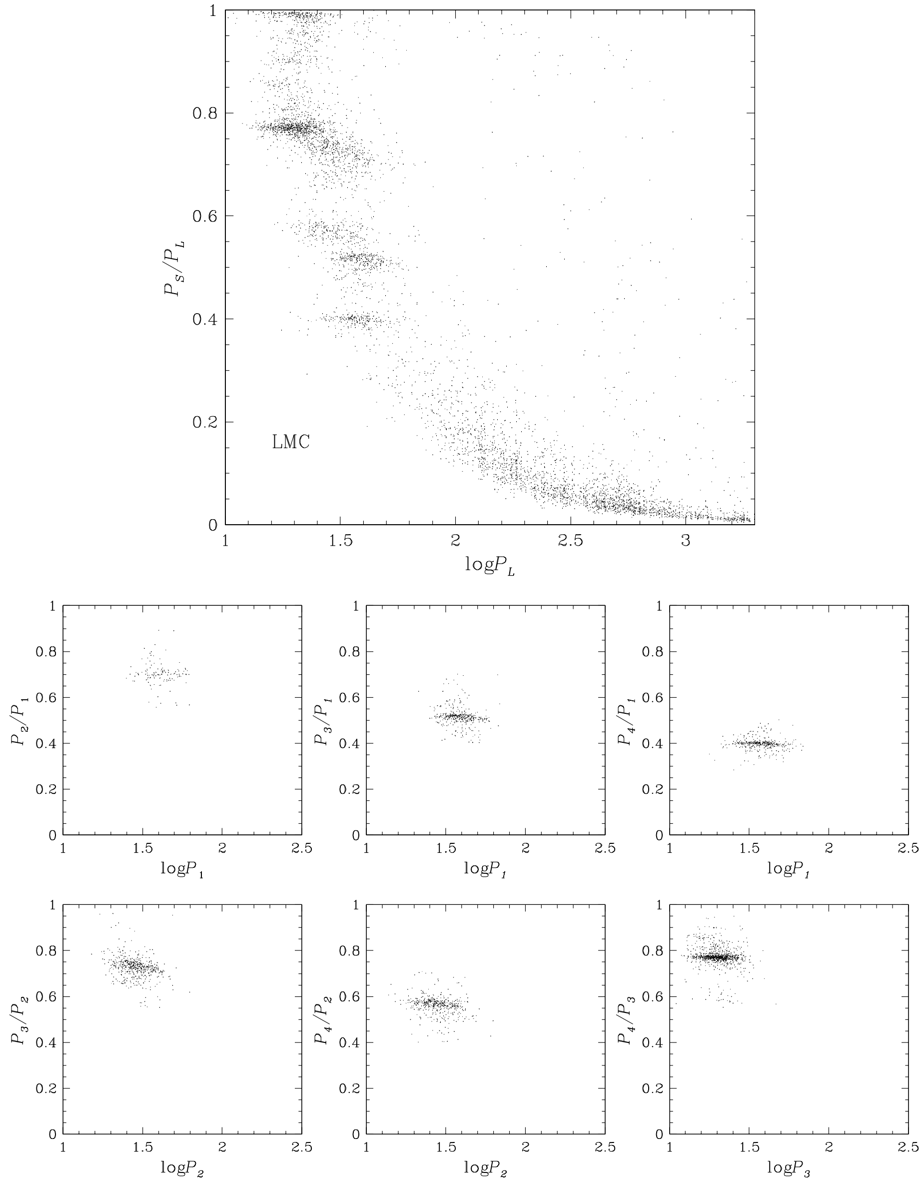

Fig. 10. Petersen diagram for OSARG stars fainter than the TRGB with one of the four dominant periods in the sequence b_4, *i.e.*, AGB stars below the TRGB.

About 2000 stars possessing the period ratios between 0.88 and 0.92, and about 1200 objects with the period ratio in the range 0.93–0.97 were found. It is not clear whether the period ratios of about 0.9 and 0.95 correspond to radial pulsations or they represent non-radial oscillations. Models of pulsating giants by Wood *et al.* (1999) permit such very close radial modes of pulsations. It should be noted that the weak signatures of these two period ratios are also seen in the Petersen diagram

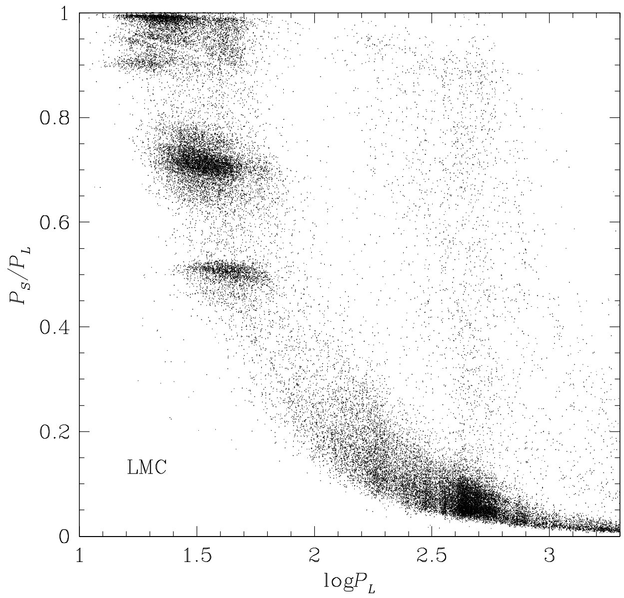

Fig. 11. Petersen diagram for OSARG stars fainter than the TRGB with one of the four dominant periods in the sequence $b_1 - b_3$, *i.e.*, RGB sample.

of the AGB sample fainter that the TRGB (Fig. 10). It can indicate that either the latter sample is still somewhat contaminated by RGB stars, or that the pulsations responsible for these period ratios can be excited in both types of giants.

6. Discussion

In this paper we presented large sample of pulsating red giants detected during the OGLE-II survey in the Magellanic Clouds. We showed that the sample can be divided into two groups with different pulsating properties. We analyzed here in detail the group of small amplitude pulsating red giants – OSARGs.

We showed that the pulsational properties of the first and second ascent OSARGs are slightly different what made it possible to show empirically that pulsating red giants fainter than the TRGB are a mixture of RGB and AGB objects and to select and extract subsamples of pulsating RGB and AGB stars fainter than the TRGB. Follow up observations of these objects could shed a new light on the differences in mechanisms of pulsation of both groups.

Knowing the properties of OSARGs in the LMC, the natural question is whether the same properties of small amplitude pulsating red giants are shared by those in other stellar systems. The most obvious candidate for the test is the SMC. Fig. 12 presents the Petersen diagram for the SMC OSARGs. Cyan dots indicate stars brighter than the TRGB while black dots those fainter than the TRGB. Additionally, the giants from the sequence b_4 are marked by the magenta dots.

It is clear that the Petersen diagram of the SMC red giants closely resembles

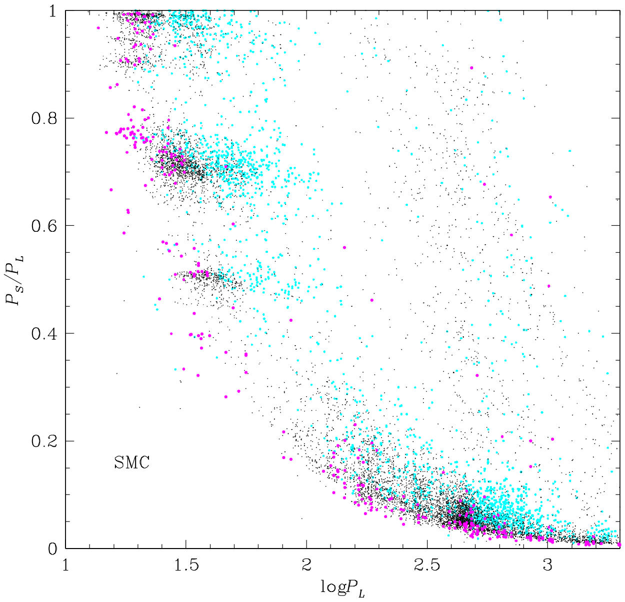

Fig. 12. Petersen diagram for OSARG stars in the SMC. Cyan dots mark OSARG stars brighter than the TRGB, black points mark RGB sample OSARGs and magenta dots OSARGs fainter than the TRGB with one of the four dominant periods in the sequence b_4, *i.e.*, AGB stars.

that of the LMC objects. The giants from the sequence b_4 form characteristic period ratio sequences coinciding with the similar sequences of type "a" OSARGs, *i.e.*, AGB stars. Therefore, similarly to the LMC we interpret those stars as AGB giants fainter than the TRGB. The sample of these stars in the OGLE-II fields is, however, relatively small. This might be related with different metallicity of both Magellanic Clouds. Certainly much larger samples of these stars will become available when OGLE-III data covering entire SMC are analyzed allowing more precise studies of SMC OSARGs. It is also worth noticing that the slopes of *PL* relations in the SMC are significantly different making these stars of little use as standard candles.

Another important stellar system to test properties of OSARGs is the Galactic bulge where Wray *et al.* (2004) discovered thousands of such objects based on the OGLE-II photometry. Unfortunately, the Galactic bulge is much worse region for analyzing the variable red giants using *PL* relations because large and likely non-standard extinction (Udalski 2003b, Sumi 2004) makes it difficult to obtain accurate intrinsic magnitudes of stars even in the IR bands. Another factor diluting the *PL* diagrams is a large geometrical depth of the Galactic bulge, *i.e.*, different distances to the Galactic bulge giants.

Fortunately the periods and amplitudes of variable giants are free of these problems. Therefore the Petersen diagram and period-amplitude diagram can be directly compared with similar ones for the MC objects. It should be, however, noted that the Galactic bulge sample was selected based on data with much shorter time-span (only three years), so that considerable fraction of periods in the Wray *et al.* (2004) list can be spurious or non-stable. Therefore, one can expect more noise in the Galactic bulge diagrams. One can also expect that because of the distance modulus smaller by about 4 mag than that of the LMC the vast majority of red giants in the OGLE-II Galactic bulge sample are stars fainter than the TRGB. The brighter objects would be saturated in the OGLE-II images.

Fig. 13 presents the Petersen diagram for the Galactic bulge red giants from the Wray *et al.* (2004) sample. All possible period ratios of the dominant periods of these stars listed by Wray *et al.* (2004) are plotted. As expected the diagram is much more noisy than the corresponding diagram for the LMC OSARG stars fainter than the TRGB – Figs. 10 and 11. Nevertheless, one can immediately notice striking similarities. The characteristic period ratios in both diagrams are identical.

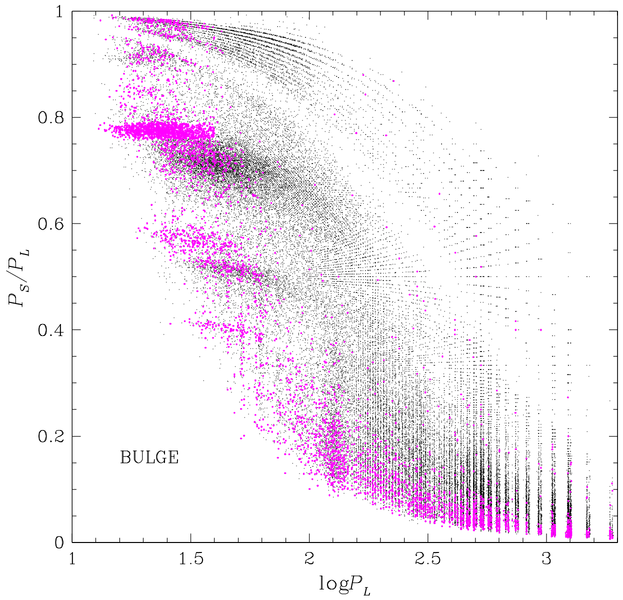

Fig. 13. Petersen diagram for OSARG stars in the Galactic bulge (Wray *et al.* 2004). Magenta dots show position of OSARG stars with period ratios corresponding to the AGB OSARG objects fainter than the TRGB in the Magellanic Clouds. Black dots mark the remaining objects, most likely RGB stars.

Because the giants from sequence b_4 cannot be extracted in the Galactic bulge with the *PL* diagram as in the Magellanic Cloud cases we selected them using the characteristic period ratio between sequences b_4 and b_3 equal to 0.76. This sequence is clearly seen in Fig. 13. Period ratios of all dominant periods of these objects are marked by magenta dots in Fig. 13.

It is striking in Fig. 13 that the selected objects populate the same sequences as the LMC OSARGs from sequence b_4, *i.e.*, the stars interpreted by us as AGB stars fainter than the TRGB (Fig. 10). The remaining giants populate sequences very similar to those of our RGB sample of LMC giants (Fig. 11). Thus, it seems justified to conclude that the small amplitude pulsating red giants in the Galactic bulge are also a mixture of both – AGB and RGB red giants and pulsational properties of these stars in the Magellanic Clouds and the Galactic bulge are very similar. Further comparison of properties of samples of these two class of giants from different environments could shed the light on the dependence of red giant pulsation mechanism on metallicity which is different in the Magellanic Clouds and Galactic bulge.

It is also possible to explain the duality in the period–amplitude diagram for small amplitude red giants discovered by Wray *et al.* (2004) in the Galactic bulge. Group A of Wray's *et al.* giants (variables with lower amplitudes and shorter periods) consists mainly of the most numerous class of OSARGs – stars in the sequence b_3. Variables in the sequence b_2 and stars brighter than the TRGB form group B of Wray's *et al.* giants in the $\log P - \log A$ diagram.

Acknowledgements. We would like to thank Dr. W. Dziembowski for careful reading of the manuscript, many important comments and suggestions. The paper was partly supported by the Polish KBN grant 2P03D02124 to A. Udalski. Partial support to the OGLE project was provided with the NSF grant AST-0204908 and NASA grant NAG5-12212 to B. Paczyński.

REFERENCES

Alard, C., and Lupton, R.H. 1998, *Astrophys. J.*, **503**, 325.
Alard, C. 2000, *Astron. Astrophys. Suppl. Ser.*, **144**, 363.
Alves, D., *et al.* 1998, in: Proc. of IAU JD24, "Pulsating Stars: Recent Developments in Theory and Observation,", Ed. Takeuti, M., and Sasselov, D.D., Universal Academic Press, Tokyo. 17
Christensen-Dalsgaard, J., Kjeldsen, H., and Mattei, J.A. 2001, *Astrophys. J.*, **562**, 141.
Cioni, M.-R.L., Marquette, J.-B., Loup, C., Azzopardi, M., Habing, H.J., Lasserre, T., and Lesquoy, E. 2001, *Astron. Astrophys.*, **377**, 945.
Dziembowski, W.A., Gough, D.O., Houdek, G., and Sienkiewicz, R. 2001, *MNRAS*, **328**, 601.
Edmonds, P.D., and Gilliland, R.L. 1996, *Astrophys. J.*, **464**, L157.
Glass, I.S., and Lloyd Evans, T. 1981, *Nature*, **291**, 303.
Groenewegen, M.A.T. 2004, *Astron. Astrophys.*, in press; astro-ph/0404561.
Henry, G.W., Fekel, F.C., Henry, S.M., and Hall, D.S. 2000, *Astrophys. J. Suppl. Ser.*, **130**, 201.
Houck, N. 1963, *Astron. J.*, **68**, 253.
Ita, Y. *et al.* 2002, *MNRAS*, **337**, L31.
Ita, Y. *et al.* 2004, *MNRAS*, **347**, 720.
Jorissen, A., Mowlavi, N., Sterken, C., and Manfroid, J. 1997, *Astron. Astrophys.*, **324**, 578.
Kiss, L.L., and Bedding, T.R. 2003, *MNRAS*, **343**, L79.
Kiss, L.L., and Bedding, T.R. 2004, *MNRAS*, **347**, L83.
Lebzelter, T., Schultheis, M., and Melchior, A.L. 2002, *Astron. Astrophys.*, **393**, 573.
Moskalik, P., Kołaczkowski, Z., and Mizerski, T. 2003, *ASP Conf. Ser.*, **310**, 498.
Noda, S. *et al.* 2002, *MNRAS*, **330**, 137.
Olech, A., *et al.* 1999, *Astron. J.*, **118**, 442.
Percy, J.R., Wilson, J.B., and Henry, G.W. 2001, *P.A.S.P.*, **113**, 983.
Stebbins, J., and Huffer, C.M. 1930, *Publ. Washburn Obs.*, **15**, 138.
Sumi, T. 2004, *MNRAS*, **349**, 193.

Udalski, A. 2000, *Acta Astron.*, **50**, 279.
Udalski, A. 2003a, *Acta Astron.*, **53**, 291.
Udalski, A. 2003b, *Astrophys. J.*, **590**, 284.
Udalski, A., Kubiak, M., and Szymański, M. 1997, *Acta Astron.*, **47**, 319.
Wood, P.R. 2000, *Publ. Astron. Soc. Aust.*, **17**, 18.
Wood, P.R., *et al.* (MACHO team) 1999, *in IAU Symp. 191*, Asymptotic Giant Branch Stars, ed. T. Le Bertre, A. Lébre, and C. Waelkens (San Francisco: ASP), 151.
Wood, P.R., Olivier, E.A., and Kawaler, S.D. 2004, *Astrophys. J.*, **604**, 800.
Wood, P.R., and Sebo, K.M. 1996, *MNRAS*, **282**, 958.
Woźniak, P.R. 2000, *Acta Astron.*, **50**, 421.
Woźniak, P.R., Udalski, M., Szymański, A., Kubiak, M., Pietrzyński, G., Soszyński, I., and Żebruń, K. 2002, *Acta Astron.*, **52**, 129.
Wray, J.J., Eyer, L., and Paczyński, B. 2004, *MNRAS*, **349**, 1059.
Żebruń, K., Soszyński, I., Woźniak, P.R., Udalski, A., Kubiak, M., Szymański, M., Pietrzyński, G., Szewczyk, O., and Wyrzykowski, Ł. 2001, *Acta Astron.*, **51**, 317.